Supporting Information

White et al. 10.1073/pnas.1403659111

SI Text

Note 1. *Ardipithecus ramidus* Dental Sample and Metrics. *Ardipithecus ramidus* variation is best documented by the dental sample from Aramis, Ethiopia, which formed the basis of our previously published studies (1, 2). This collection comprises 65 cataloged specimens that represent portions of the crown and roots, ranging from relatively intact tooth rows to merely small fragments of tooth. These specimens are listed in the supplementary materials of ref. 1, and crown dimension statistics and comparisons were presented in the supplementary materials of ref. 2.

Here, in Tables S1 and S2, we provide the tooth-by-tooth crown dimension metrics of 34 individual specimens, totaling 101 crowns, not counting antimeres. When antimeres were available, the metric of the better-preserved side was used. In Tables S3 and S4, we provide the detailed size and shape metrics of 16 *Ar. ramidus* canines, results previously presented in the supplementary materials of ref. 2. Another six canines were evaluated in terms of size by other comparisons, also detailed in the supplementary materials of ref. 2.

Note 2. Original Length of the ARA-VP-6/500 Right Tibia. Accurate estimation of tibial length is important in determining the limb proportions of the ARA-VP-6/500 "Ardi" specimen. Relative to her tibia, Ardi's arm bones are shorter than in extant great apes. Some have questioned the accuracy of our published tibial length estimate, perhaps influenced by expectations about limb proportions based on living great ape models or perhaps because our published photographs of the skeleton did not comprehensively show the damage to the original fossil.

We reported in the supplementary information of ref. 3 that the ARA-VP-6/500 tibia was "...complete including the intercondylar process but lacks a portion of its medial malleolus." This explanatory notation was offered in the context of introducing our original conservative length estimate of 262 mm + 2 mm. However, it has led to some confusion because it is possible to read that text to mean that a portion of the medial malleolus had been preserved. It is entirely absent, including its typical contribution to the medial side of the distal joint surface.

Although the shaft is relatively intact, both proximal and distal ends of the tibia have suffered crushing, with loss of bone. The distal end of the tibia, including the entire plafond, is completely absent. There is no remaining part of the joint surface or the distal-most shaft. Our estimate of the undamaged original length of this tibia took these facts into account. Figs. S2 and S3 provide detailed illustration essential for accurate length estimation.

Note 3. The most important similarities between the pelvis of *Ar. ramidus* and *Australopithecus* (4, 5) are depicted in Fig. S4, comparing ARA-VP-6/500 (*Ar. ramidus*) and A.L.288–1 (*Australopithecus afarensis*).

1. White TD, et al. (2009) *Ardipithecus ramidus* and the paleobiology of early hominids. *Science* 326(5949):75–86.
2. Suwa G, et al. (2009) Paleobiological implications of the *Ardipithecus ramidus* dentition. *Science* 326(5949):94–99.
3. Lovejoy CO, Suwa G, Simpson SW, Matternes JH, White TD (2009) The great divides: *Ardipithecus ramidus* reveals the postcrania of our last common ancestors with African apes. *Science* 326(5949):100–106.
4. Lovejoy CO, Suwa G, Spurlock L, Asfaw B, White TD (2009) The pelvis and femur of *Ardipithecus ramidus*: The emergence of upright walking. *Science* 326(5949):71e1–71e6.
5. Lovejoy CO (2005) The natural history of human gait and posture. Part 1. Spine and pelvis. *Gait Posture* 21(1):95–112.

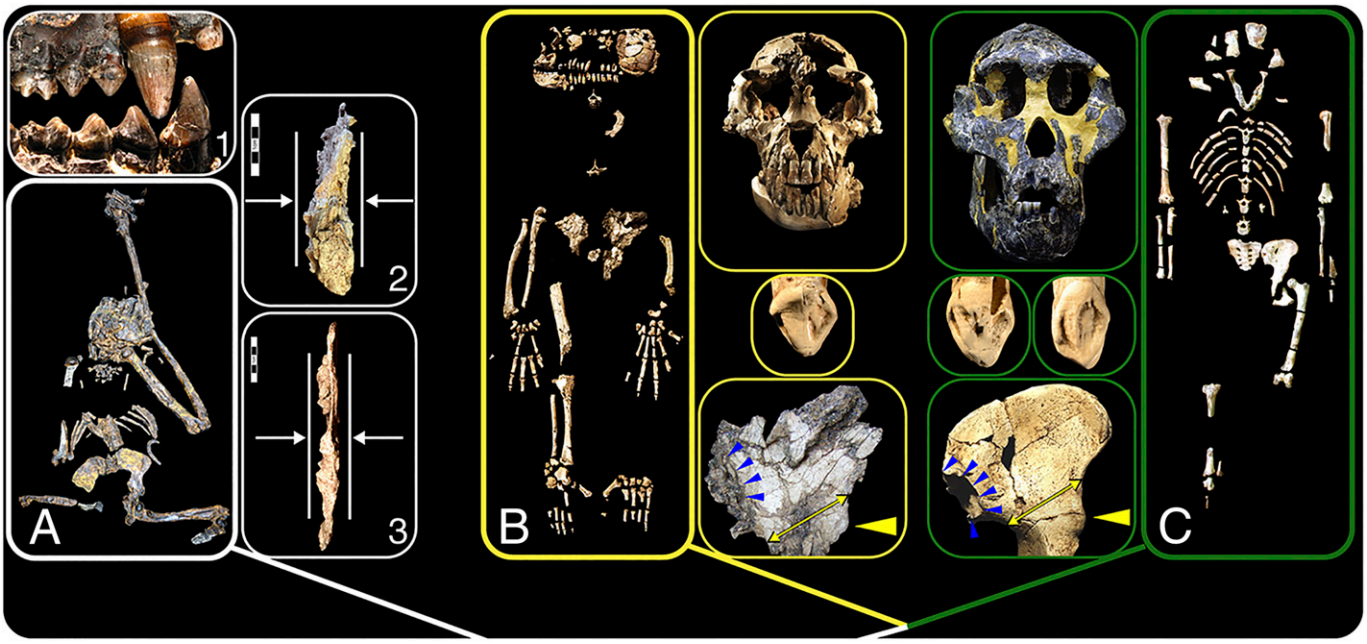

Fig. S1. *Oreopithecus* does not confuse phylogenetic placement. The single skeleton of *Oreopithecus* (*A*, cast) was crushed flat. Much of its true anatomy is difficult or impossible to ascertain. Despite this difficulty, some have asserted that it shares extraordinary parallelisms with hominids, thereby undermining the reliability of phylogenetically positioning *Ardipithecus*. Primary among such claims is the assertion of a nonhoning C/P_3 complex, obviously falsified by *A, 1* (upper BAC60 and lower IGF11778 dentitions scaled to comparable length and reversed). The sharp, projecting upper canine is steeply honed. Another claim is an anteriorly situated foramen magnum. However, the anterior view (*A, 2*) shows the skull to have been geologically flattened and fragmented, with key pieces displaced so that no observations support this claim (arrows indicate direction of crushing; maximum crushed breadth is a mere ~30 mm; scale in centimeters). A third claim is that *Oreopithecus* exhibits a discrete anterior inferior iliac spine as in hominids (AIIS; yellow triangles in *B* and *C*). The existence of such a feature in *Oreopithecus* is indeterminate, as illustrated by a lateral view of the dorsoventrally flattened pelvis (*A, 3*). The protrusion above its acetabulum is partly an artifact of preparation, bearing no topographic or surface morphologic resemblance to the highly derived AIIS of hominids (*SI Text*, *Note 3*). A fourth claim is that *Oreopithecus* has a short broad ilium. In fact, its isthmus (lower iliac blade) appears primitively narrow and tall. Upper iliac "shortness" is a mere illusion caused by the bone fossilized between the ilia. However, that bone is a dislodged and displaced lumbar, not a sacral vertebra (*A*). Therefore, the main claimed *Oreopithecus*-hominid "parallelisms" are all falsified or dubious. In contrast, each of the independently derived character complexes of the *Ardipithecus* dentition, cranium, and pelvis includes multiple homologous characters exclusively shared with other hominids. The boxes in *B* show *Ar. ramidus*: ARA-VP-6/500 Ardi skeleton, its cranial stereolithograph, a presumed male upper canine (largest known in the species sample, ARA-VP-1/1818), and the ARA-VP-6/500 ilium (blue arrowheads indicate preserved anterior margin of sacral articular surface; this margin extended more inferiorly by an indeterminate amount before crushing and bone loss). The boxes in *C* show *Au. afarensis;* A.L. 288–1 Lucy skeleton (*Right*); the more complete skull of another small conspecific [(*Upper Left*) A.L. 822–1, courtesy of William Kimbel, Insitute of Human Origins, Tempe, AZ]; the largest little-worn *Au. anamensis* and *Au. afarensis* upper canines known (*Middle Left* and *Middle Right*, respectively); and the A.L. 288–1 ilium (blue arrowheads indicate sacral articular margin, crushing of posterior margin uncorrected).

Fig. S2. Lateral views of *Ar. ramidus* and *Pan troglodytes* right tibiae. (*A*) Photograph of a chimpanzee tibia whose total length is 264 mm. This corresponds to the upper limit for the length that we originally estimated (262 + 2 mm) for the Ardi fossil tibia. (*B*) Photograph of a cast of the ARA-VP-6/500 tibia. The proximal end of the fossil suffered some crushing, with compression and posterodistal rotation of the tibial plateau best seen in this view. This very likely decreased the overall length, but it is difficult to estimate by how much. We have conservatively not attempted to correct for this possible proximal shortening. The ARA-VP-6/500 tibia shows no evidence of the morphological features that ubiquitously occur near the (here entirely absent) plafond. Taking the bone loss and crushing into account, the ARA-VP-6/500 tibia's length estimate was made based on direct anatomical comparisons with human and chimpanzee tibias. A small (~1 cm length) portion of adherent, presumably diagenetically displaced cortical bone was initially present on the disto-lateral extent of the preserved fossil and appears in previous photographs of the original specimen (and blue arrowhead in *B*). Because this artificially displaced fragment might be misinterpreted as a morphological "feature" by those viewing/measuring only casts or photos, we removed it from the original fossil in 2012, revealing (as expected) only ordinary, unremarkable subperiosteal shaft bone beneath it.

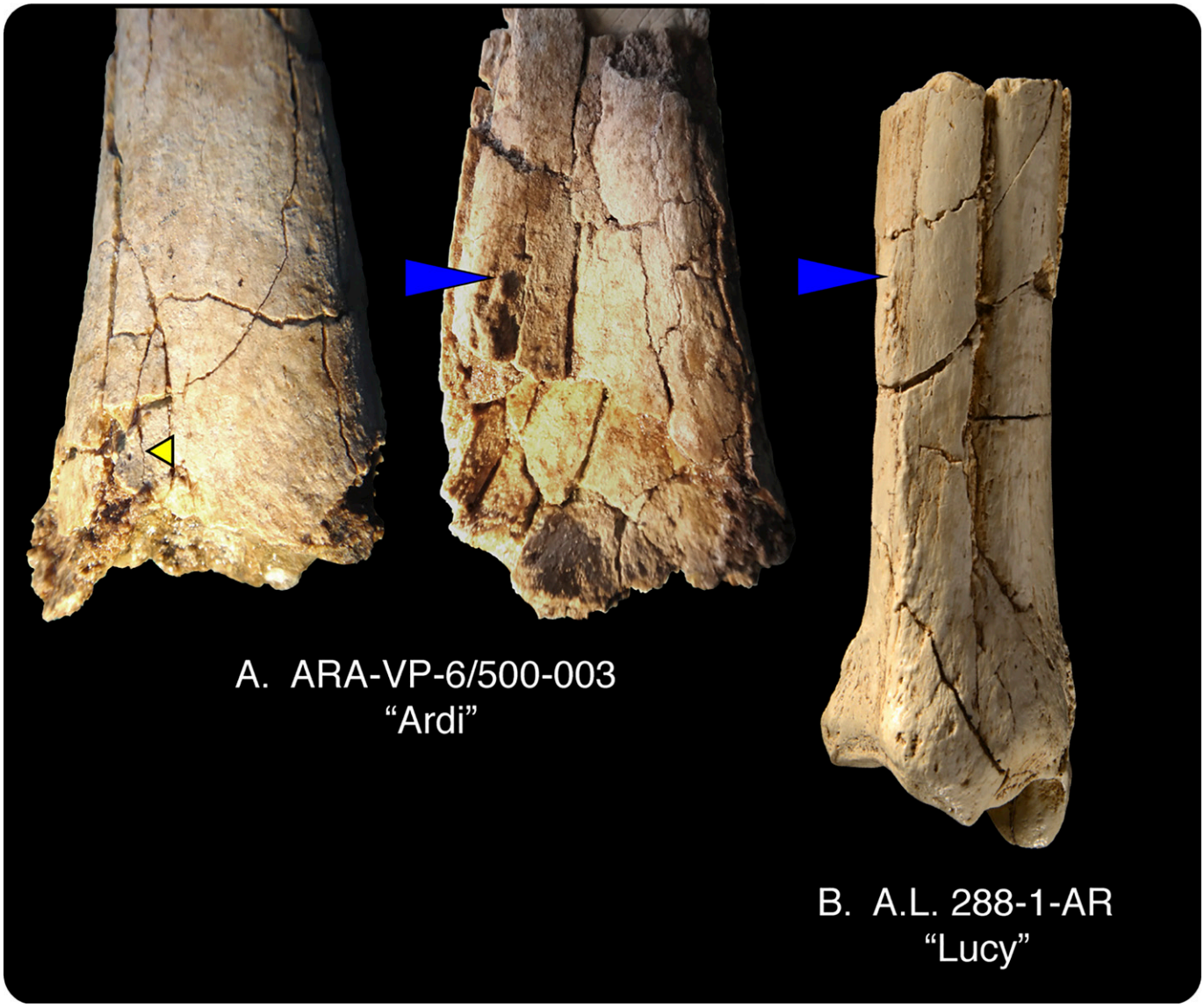

Fig. S3. Crushing and bone loss on the original *Ar. ramidus* distal tibia (ARA-VP-6/500), compared with a small *A. afarensis* distal tibia (cast). (*A*) Posterior (*Left*) and anterior (*Right*) views of ARA-VP-6/500. (*B*) A.L. 288–1 Lucy distal tibia, posterolateral view. The preserved distal shaft of the Ardi tibia was crushed in a mostly anteroposterior direction. Failure to appreciate this distortion and bone loss could result in inaccurate and misleading tibia length estimates. The anteroposterior crushing has artificially accentuated the medial and lateral flare of the fossil's distal shaft. The shaft in its original uncrushed condition was likely only gradually expanding in the region viewed. In undistorted ape and human tibiae, such gradual shaft expansion differs from the stronger, more distinct distal flare closer to the distal joint surface (plafond, see Fig. S2). Beyond the distortion of the fossil, there is no evidence for such dramatic distal flare in the Ardi tibia. The corresponding section of the distal shaft/metaphyseal junction was broken away and is now entirely missing. There are two areas preserving potentially useful surface anatomy proximal to the Ardi tibia's broken end. The first is a subtle surface depression (yellow triangle) that might have been contacted by the tendon of the tibialis posterior. This depression lies in a region where the surface bone is multiply fragmented. A palpable wide, smooth, shallow groove may have occurred, but there are no elevated margins. The second feature is a small rugosity possibly associated with the proximal initiation of the tibiofibular syndesmosis (blue pointer). Neither feature contradicted our adopted length estimate. The figure illustrates alignment of the Ardi and Lucy tibiae based on the proximal ends of the possibly homologous bony rugosities. If these positions were comparable relative to total tibial length, then the ARA-6/500 tibia would have been significantly longer than our original estimate (Fig. S2). However, because of extensive variation in these bony features, we chose not to use this landmark in estimating ARA-6/500 tibia length. Rather our length estimate remains more conservative. Thus, any residual uncertainty resulting from crushing and bone loss has only a minimal effect (a few millimeters) on any biological inferences made from this fossil tibia's estimated length.

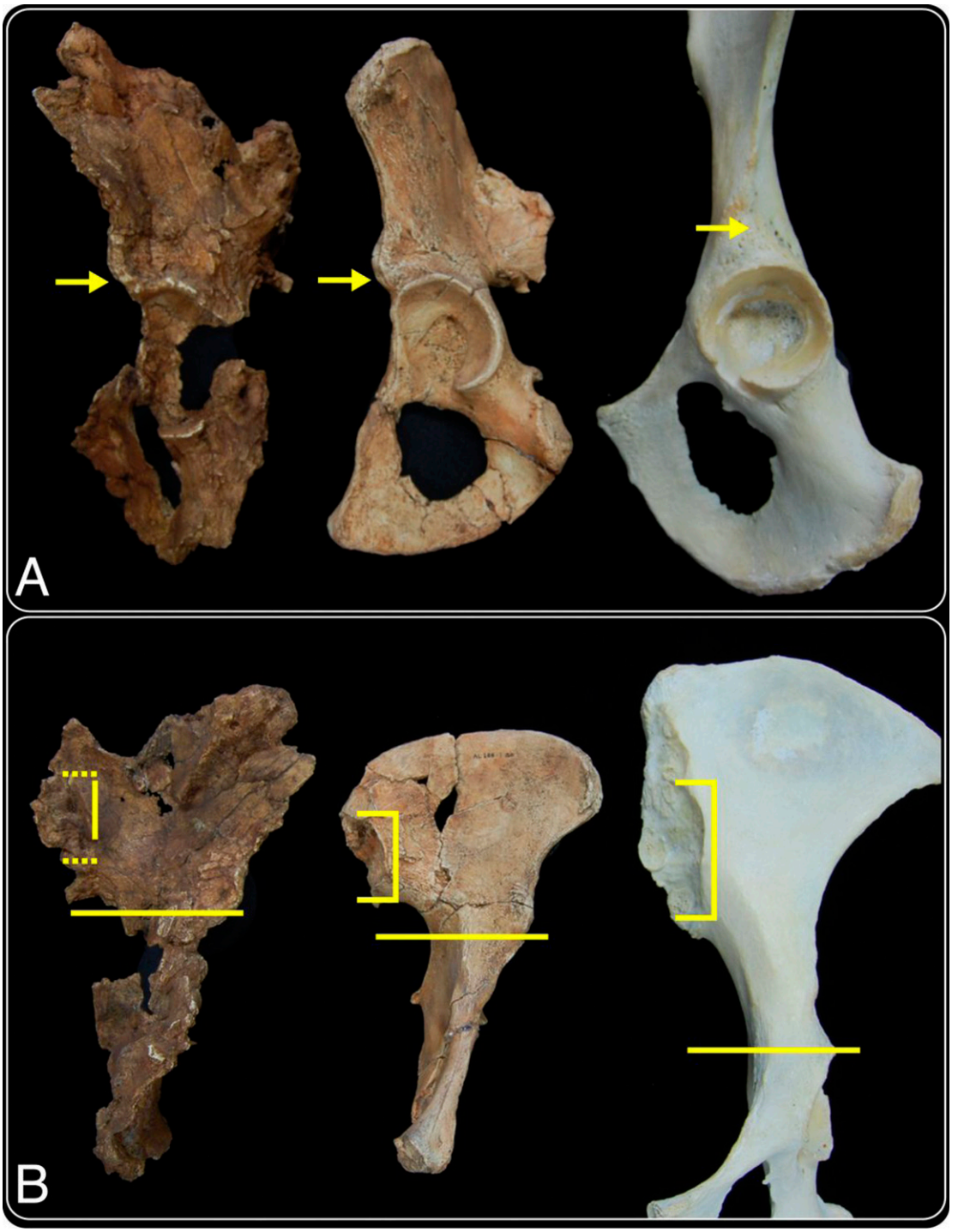

Fig. S4. The ilia of *Ar. ramidus* and *Australopithecus* share important derived features. *Os coxae* aligned as follows in *A* and *B*: (*Left*) *Ar. ramidus* ARA-VP-6/500 "Ardi" (cast); (*Center*) *Au. afarensis* A.L. 288–1 Lucy (cast); (*Right*) modern chimpanzee. In *A*, arrows point to placement of the lateral margin of the iliac blade relative to the acetabulum. This junction is anteriorly displaced in Ardi and Lucy, resulting in an inferior iliac blade that is wide and dramatically "twisted" (faces more toward the sagittal plane). A well-developed anterior inferior iliac spine (AIIS) occurs at this site in both hominid specimens. Note that the vertical diameter of the Ardi acetabulum has been artificially exaggerated by extensive matrix-filled expansion cracking. The AIIS is placed immediately above the acetabulum, and forms a localized thick protuberance that terminates abruptly superiorly. It is distinctly curved (medially convex) in anterior view, and is flanked by a localized concavity on the lateral iliac surface just above the acetabular margin. This morphological complex is commonly seen in *Australopithecus* and later hominids, likely reflecting the separate ossification center of the hominid AIIS. In *B*, brackets show the superior and inferior extents of the sacral articular surface (auricular). The extremities of the Ardi articulation cannot be established with certainty (because of crushing and bone loss). The solid line shows the projected vertical extent of the preserved anterior margin. Based on angulation of the auricular surface with the adjacent iliac fossa and degree of protrusion of the anterior margin, the original (undamaged) superior extent of the auricular was probably at or close to its preserved upper extent. Conversely, it is difficult to evaluate how much more posteroinferiorly the auricular might have extended (lower dotted line). Regardless of these uncertainties, it is clear that compared with the chimpanzee (and all known Miocene and living apes), the projected vertical distance between the acetabulum (horizontal line indicates its upper margin) and the auricular surface is distinctly short in both the Ardi and Lucy ilia. The above constellation of features, shared by Ardi and Lucy, represents an important part of the hominid upper pelvis that enables efficient pelvic control and full extension of the knee and hip during bipedal locomotion (see refs. 4 and 5 for further details). The *Ar. ramidus* ilium thus preserves and provides direct evidence of these early hallmarks of upright bipedality.

Table S1. Individual tooth crown metrics of Aramis *Ardipithecus ramidus*: Upper dentition

	UI1		UI2		UC			UP3			UP4		UM1		UM2		UM3	
Specimen no.	MD	BL	MD	BL	MD	MXOB	HT	MXMD	BL	HT	MD	BL	MD	BL	MD	BL	MD	BL
ARA-VP-1/1																	10.2	12.3
ARA-VP-1/2		8.2																
ARA-VP-1/127						10.9												
ARA-VP-1/300	9.9	7.7	6.9	7.5	11.2	11.1	14.5	8.0	12.4	9.7	8.0	11.9	10.4	11.9	11.7	14.6	11.0	14.3
ARA-VP-1/400															12.1	14.4		
ARA-VP-1/703								6.7	10.4									
ARA-VP-1/1814															12.0	13.8		
ARA-VP-1/1818		8.1	7.4	8.0	11.9	12.2	14.9	7.9	12.0	9.1	8.0	12.0	10.8	13.0	12.5	15.3	12.1	15.3
ARA-VP-1/1875															12.8	14.6		
ARA-VP-1/1900						11.6												
ARA-VP-1/2645													9.8	11.2		13.3		
ARA-VP-1/3288													10.8	11.8				
ARA-VP-1/3289						9.9												
ARA-VP-1/3292		7.1																
ARA-VP-6/1	10.0	7.5			11.5	11.7	14.6	8.4	12.5	10.5	8.4	11.3			11.8	14.1		
ARA-VP-6/500			6.3	6.8							7.2	11.3	10.0	11.4	11.0	13.4	11.2	13.5
ARA-VP-6/502													10.5	11.5				
ARA-VP-17/1						11.3						11.4	11.1					
KUS-VP-2/100						11.3					7.5		10.5	11.8				
KUS-VP-2/154								7.6	11.3		7.5	11.7	10.3	12.1	12.0	14.2		
SAG-VP-7/118				7.8	11.2	11.7		7.7	11.8	8.8	7.5	11.8						

All values are in millimeter and corrected for wear and/or damage when necessary. Right side was measured when both sides were equally well-preserved. See Suwa et al. (2) and *SI Text* for further details. BL, buccolingual diameter; C, canine; HT, labial or buccal crown height adjusted for minor wear; I, incisor; M, molar; MD, mesiodistal diameter; MXMD, maximum mesiodistal diameter; MXOB, maximum oblique crown diameter; P, premolar; U, upper. KUS-VP-2/154 has an upper di1, MD, 7.0 mm; BL, 4.5 mm.

Table S2. Individual tooth crown metrics of Aramis *Ardipithecus ramidus*: Lower dentition

	LI1		LI2		LC			LP3			LP4		LM1		LM2		LM3	
Specimen no.	MD	BL	MD	BL	MXOB	PP	HT	MXOB	PP	HT	MD	BL	MD	BL	MD	BL	MD	BL
ARA-VP-1/128				6.6	11.1			10.0	7.4		7.5	9.5	11.2	10.3	13.0	11.9	12.7	11.0
ARA-VP-1/129	6.0																	
ARA-VP-1/200													11.0	10.3				
ARA-VP-1/300	5.7	6.4	7.2	7.6	12.1	10.5	16.6	10.9	8.1	10.0	8.3	10.2	11.4	10.4	13.7	12.5	13.2	13.1
ARA-VP-1/401		6.1		7.0	10.6	8.2		9.2	7.0		8.0	9.0	11.2	10.8			11.3	10.4
ARA-VP-1/1815					11.8	9.5												
ARA-VP-1/3291													11.8					
ARA-VP-6/1								11.5	8.2	11.0	8.9	9.7						
ARA-VP-6/500	5.4	6.1	6.4	7.5	10.3	8.0	14.4	9.6	7.2	9.5	7.6	9.6	11.0	10.5	12.6	12.3	13.0	12.6
ARA-VP-6/514											7.3	9.1						
ARA-VP-6/1010								9.4	7.2	9.8								
ARA-VP-6/1011	5.2	5.8																
ARA-VP-6/1640								9.9	7.3	9.8								
KUS-VP-2/102													12.5	11.5				
KUS-VP-2/103																		12.5
KUS-VP-2/154															14.1	12.2		
SAG-VP-7/225															12.5	11.8	11.6	11.4

All values are in millimeter and corrected for wear and/or damage when necessary. Right side was measured when both sides were equally well-preserved. See Suwa et al. (2) and *SI Text* for further details. BL, buccolingual diameter; C, canine; HT, labial or buccal crown height adjusted for minor wear; I, incisor; L, lower; M, molar; MD, mesiodistal diameter; MXOB, maximum oblique crown diameter; P, premolar; PP, maximum diameter perpendicular to MXOB. ARA-VP-1/129 has a lower dm1, MD, 7.3 mm; BL, 4.9 mm.

Table S3. *Ardipithecus ramidus* and other canine crown and root metrics: Upper canine

Specimen no.	Taxon	UCMAX	UCMD	UCBL	UCMXOB	UCPP	UCHT	UCMCLT	UCDCLT	Root MXOB	Root PP	Root HT
ASK-VP-3/400	*Ar. kadabba*	(11.8)	11.8				[15.5] ((16-16.5))	10.5	9.9			
ARA-VP-1/127	*Ar. ramidus*	(10.9)		10.7	10.9					10.4	7.6	
ARA-VP-1/300	*Ar. ramidus*	(11.2)	(11.2)	11.0	11.1	(11.2)	14.5	9.1	9.0	10.9	8.7	
ARA-VP-1/1818	*Ar. ramidus*	(12.2)	11.9	11.9	(12.2)	10.9	(14.9)	(10.0)	(9.0)	12.2	9.2	25.2
ARA-VP-1/1900	*Ar. ramidus*	(11.6)		(11.4)	(11.6)	(10.4)				(11.4)	(8.8)	34.9
ARA-VP-1/3289	*Ar. ramidus*	(9.9)		9.8	9.9	8.4				9.8	7.8	
ARA-VP-6/1	*Ar. ramidus*	11.7	11.5	11.5	11.7	11.1	14.6	7.5	9.1			
ARA-VP-6/500	*Ar. ramidus*						((13-13.5))			((9.7–10.0))	7.4	(24.5)
ARA-VP-17/1	*Ar. ramidus*	(11.3)		11.3	11.3	10.0				11.1	8.7	29.1
KUS-VP-2/100	*Ar. ramidus*	(11.3)		10.8	11.3	10.0				11.2	9.3	27.3
SAG-VP-7/118	*Ar. ramidus*	11.7	(11.2)	10.7	11.7	10.2				11.3	9.2	31.0
ASI-VP-2/2	*Au. anamensis*	11.8	(11.5)	10.9	11.8	10.1				10.7	8.8	24.1
ASI-VP-2/334	*Au. anamensis*	12.4	12.3	11.8	12.4	10.8				11.9	9.8	(24.0)
ASI-VP-2/367	*Au. anamensis*	(10.3)	(10.0)	(9.1)	(10.3)	(8.6)	(13.6)	(7.2)	(8.0)			
KNM-KP 35839	*Au. anamensis*	11.6	11.6	10.8	11.2	9.2	(15.4)	10.2	10.0			
L.H.-6	*Au. afarensis*	(10.5)	(10.5)	10.0	10.2		13.4	8.0	(9.0)			
A.L. 333x-3	*Au. afarensis*	11.6	10.4	11.5	11.6	9.6	(16.2)	6.4	9.4	11.2	8.4	(25.5)
A.L. 400–1b	*Au. afarensis*	10.5	9.2	10.3	10.5	9.1				10.1	6.7	19.4

BL, buccolingual diameter perpendicular to MD; DCLT, distal crest length (from cusp tip to shoulder corner); HT, labial height from cervix to crown (or root) tip adjusted for minor wear; MCLT mesial crest length (from cusp tip to shoulder corner); MD, mesiodistal diameter across crown shoulders; MXOB, maximum oblique buccolingual diameter; PP, maximum diameter perpendicular to MXOB; UC, upper canine; MAX is larger of MD and MXOB. Root-MAXOB and Root-PP taken at cervix. ( ): estimated diameter, corrected for wear and damage; [ ]: damaged, worn or incompletely developed diameter as preserved (not used in statistical analysis); (( )): rough estimation (not used in statistical analysis).

Table S4. *Ardipithecus ramidus* and other canine crown and root metrics: Lower canine

Specimen no.	Taxon	LCMD	LCBL	LCMXOB	LCPP	LCHT	LCMCLT	Root MXOB	Root PP	Root HT
ALA-VP-2/10	*Ar. kadabba*			11.2	7.8	[13.4] ((14.5–15.5))		11.1	7.1	
STD-VP-2/61	*Ar. kadabba*			10.8	7.8	14.6	7.6	10.4	7.3	
ARA-VP-1/128	*Ar. ramidus*		11.0	11.1				10.9	8.4	25.2
ARA-VP-1/300	*Ar. ramidus*	(10.8)	10.6	12.1	10.5	16.6	(8.4)	11.6	8.8	
ARA-VP-1/401	*Ar. ramidus*	8.2	10.2	10.6	8.2			10.2	7.8	26.0
ARA-VP-1/1815	*Ar. ramidus*	(10.3)	10.6	11.8	(9.5)			12.2	9.5	31.4
ARA-VP-1/3293	*Ar. ramidus*							(9.8)	(7.4)	
ARA-VP-6/500	*Ar. ramidus*			(10.3)	(8.0)	(14.4)	(6.5)	10.1	7.2	25.0
ASI-VP-2/3	*Au. anamensis*			(10.3)				(10.5)	(7.6)	24.7
KNM-KP 29286	*Au. anamensis*	10.4	11.0	12.1	9.6	(15.4)	(7.0)			
A.L. 333w-10	*Au. afarensis*		12.0	12.0				11.9	7.8	23.8
A.L. 333–90	*Au. afarensis*		9.7	10.8				10.6	8.0	20.6

BL, buccolingual diameter perpendicular to MD; HT, labial height from cervix to crown (or root) tip adjusted for minor wear; LC, lower canine; MCLT mesial crest length (from cusp tip to shoulder corner); MD, mesiodistal diameter across crown shoulders; MXOB, maximum oblique buccolingual diameter; PP, maximum diameter perpendicular to MXOB. Root-MAXOB and Root-PP taken at cervix. ( ): estimated diameter, corrected for wear and damage; [ ]: damaged, worn or incompletely developed diameter as preserved (not used in statistical analysis); (( )): rough estimation (not used in statistical analysis).